



Formation of supermassive black holes in galaxies through collisions in Nuclear Star Clusters

M. Liempi¹, A. Benson², A. Escala³, D.R.G. Schleicher¹ & L. Almonacid¹

¹ *Departamento de Astronomía, Universidad de Concepción, Chile*

² *Carnegie Observatories, EE.UU.*

³ *Departamento de Astronomía, Universidad de Chile, Chile*

Received: 09 February 2024 / Accepted: 23 April 2024

©The Authors 2024

Resumen / En el centro de las galaxias se observan cúmulos nucleares de estrellas y/o agujeros negros supermasivos. Aunque cada objeto se encuentran en diferentes regímenes, es posible detectar ambos coexistiendo en galaxias con masas estelares $\sim 10^{10} M_{\odot}$. En este trabajo, presentamos la implementación de un modelo de formación y evolución de cúmulos de estrellas nucleares en GALACTICUS, un código semianalítico diseñado para simular la formación y evolución de galaxias. Nuestro objetivo es explorar el papel de cúmulos durante la formación de los agujeros negros. Suponemos un escenario de formación estelar in-situ en el gas acumulado en el centro de la galaxia. Además, introducimos un modelo de colapso de los cúmulos, donde finalmente colapsan en una semilla de agujero negro al alcanzar una masa crítica donde las colisiones entre estrellas son relevantes dentro del cúmulo. Esta masa crítica se alcanza cuando la escala de tiempo de colisiones es más corta que la edad del sistema. Al explorar este escenario de colapso, nuestro objetivo es encontrar pistas sobre las posibles implicaciones en la población de agujeros negros. Nuestra investigación profundiza en como este escenario de colapso puede afectar la población general de agujeros negros, así como las conexiones entre el cúmulo, la galaxia anfitriona y el agujero negro central. En nuestros resultados encontramos la formación de semillas con masas entre $10^3 - 10^5 M_{\odot}$ a partir de este mecanismo.

Abstract / Nuclear Star Clusters (NSCs) and/or Supermassive Black Holes (SMBHs) are observed in the center of galaxies. Although each object is found in different regimes, it is possible to find both of them coexisting in galaxies with stellar masses $\sim 10^{10} M_{\odot}$. In this work we present an implementation of a NSC model in GALACTICUS, a semi-analytic code designed for simulating galaxy formation and evolution. Our focus is exploring the role of NSCs during the formation of SMBHs. We assume an in situ star formation scenario in the gas accumulated in the center of the galaxy. Moreover, we introduce a collapse model for NSCs, where they ultimately collapse into a BH seed upon reaching a critical mass for which collisions between stars become relevant within the cluster. This critical mass is reached when the collisional timescale is shorter than the age of the system. By exploring this collapse scenario, we aim to shed light on its potential implications for the resulting population of SMBHs. Our investigation delves into how this collapse scenario can impact the overall SMBH, as well as the intricate connections between NSCs, galaxies, and SMBHs. This research provides insights into the formation and evolution of NSCs and their impact on the galactic and black hole environments. We find the formation of BH seeds with masses in the range $10^3 - 10^{5.5} M_{\odot}$.

Keywords / black hole physics — galaxies: nuclei — methods: analytical

1. Introduction

Nuclear Star Clusters (NSCs) are located in the center of a large fraction of early- and late-type galaxies (e.g., Phillips et al., 1996; Durrell, 1997; Böker et al., 2002, 2004; Côté et al., 2006; Georgiev et al., 2009; Neumayer et al., 2011; Hoyer et al., 2021). Different methods for the estimation of their mass suggest masses in the range of $10^4 - 10^9 M_{\odot}$. Similarly, it is possible to observe Supermassive Black Holes (SMBHs) in the center of almost all the massive galaxies (Kormendy & Ho, 2013) with masses of $10^6 - 10^{10} M_{\odot}$ (Natarajan & Treister, 2009; Gültekin et al., 2009; Volonteri, 2010; Rusli et al., 2013; Pacucci et al., 2017).

Both objects scale alike with global properties of the host galaxy (e.g. Georgiev et al., 2016). NSCs hold

correlations between their mass and the host-galaxy bulge luminosity, mass and velocity dispersion (Ferrarese et al., 2006; Wehner & Harris, 2006; Erwin & Gadotti, 2012). On the other hand, the masses of SMBHs correlate with the host spheroid including luminosity, mass, and velocity dispersion (Seth et al., 2008; Kormendy & Ho, 2013; Reines & Volonteri, 2015; Bentz & Manne-Nicholas, 2018). These scaling relations are slightly different in early- and late-type hosts (Erwin & Gadotti, 2012), suggesting a common physical mechanism responsible for the formation of NSCs and/or SMBHs in the galactic center. This mechanism remains unclear.

Moreover, in galaxies with stellar mass around $\sim 10^{10} M_{\odot}$ there are observations of NSCs surrounding SMBHs (Filippenko & Ho, 2003; Seth et al., 2008, 2010;

Neumayer & Walcher, 2012; Nguyen et al., 2019), and the coexistence of both objects might suggest that NSCs have a role in the formation of SMBHs.

Escala (2021) demonstrated that observed NSCs are in a regime where collisions are not relevant throughout the system and SMBHs are found in regimes where collisions between stars are expected to be dynamically relevant. In this sense, NSCs in virial equilibrium with short collision times will collapse toward the formation of a massive black hole.

2. Methodology

In this work we implement an in-situ NSC formation model in GALACTICUS, a semi-analytic model for galaxy formation and evolution (Benson, 2012) to explore the space of parameters related to the model.

We also implement a recipe for BH seed formation in NSCs based on the work of Escala (2021), and Vergara et al. (2023).

2.1. The model

In this scenario, we assume NSCs may form by star formation in the gas accumulated in the center of the galaxy. The gas is accumulated in a nuclear reservoir correlated to the star formation events in the bulge (Granato et al., 2004; Haiman et al., 2004; Lapi et al., 2014; Antonini et al., 2015; Neumayer et al., 2011) by

$$\dot{M}_{\text{NSC}}^{\text{gas}} = A_{\text{res}} \dot{M}_{\text{spheroid}}^{\text{stellar}}, \quad (1)$$

where $\dot{M}_{\text{spheroid}}^{\text{stellar}}$ is the star formation in the bulge and A_{res} is a free parameter in the order of $\sim 10^{-2} - 10^{-3}$ (Antonini et al., 2015).

The size of the NSC is assumed to scale with the square root of the dynamical mass of the system,

$$r_{\text{NSC}} = r_0 \sqrt{\frac{M_{\text{NSC}}^{\text{dyn}}}{10^6 M_{\odot}}}, \quad (2)$$

where r_0 is the mean radius of the observed NSCs set equal to $r_0 = 3.3$ pc (Neumayer et al., 2020), and $M_{\text{NSC}}^{\text{dyn}} = M_{\text{NSC}}^{\text{gas}} + M_{\text{NSC}}^{\text{stellar}}$. We use a Sérsic profile with index $n = 2.28$ for the mass distribution of the NSCs. While this is quite arbitrary, we choose this value based on the results of Pechetti et al. (2020) where density profiles for 29 galaxies containing NSCs in a volume-limited survey are analyzed.

The star formation rate in the NSC gas reservoir follows the prescription of Krumholz et al. (2009) in a quiescent mode as in the model of Sesana et al. (2014) and Antonini et al. (2015),

$$\dot{M}_{\text{NSC}}^{\text{stellar}} = f_c \frac{M_{\text{NSC}}^{\text{NSC}}}{t_{\text{SF}}}, \quad (3)$$

where f_c is the fraction of the cold gas of the NSC available for the star formation, $M_{\text{NSC}}^{\text{gas}}$ is the gas of the NSC and t_{SF} is the timescale on star formation takes place.

The fraction of the cold gas f_c available to form stars depends on the metallicity, at high metallicities ($Z > 0.01 Z_{\odot}$) the fraction f_c is determined by the molecular gas, whereas at lower metallicities ($Z < 0.01 Z_{\odot}$), star

formation takes place in the atomic phase (Krumholz, 2012),

$$f_c = \max \left(0.02, 1 - \left[1 + \left(\frac{3}{4} \frac{s}{1 + \delta} \right)^{-5} \right]^{-1/5} \right), \quad (4)$$

with

$$s = \frac{\ln(1 + 0.6\chi)}{0.04\Sigma_1 Z}, \quad (5)$$

$$\chi = 0.77(1 + 3.1Z^{0.365}), \quad (6)$$

$$\delta = 0.0712(0.1s^{-1} + 0.675)^{-2.8}, \quad (7)$$

$$\Sigma_1 = \frac{\Sigma_{\text{res}}}{M_{\odot} \text{ pc}^{-2}}, \quad (8)$$

$$\Sigma_{\text{res}} = \frac{M_{\text{NSC}}^{\text{gas}}}{4\pi r_{\text{NSC}}^2}. \quad (9)$$

The timescale is obtained assuming that star formation happens in clouds (Krumholz et al., 2009; Sesana et al., 2014; Antonini et al., 2015) and is given by

$$t_{\text{SF}}^{-1} = (2.6 \text{ Gyr})^{-1} \times \begin{cases} \left(\frac{\Sigma_{\text{res}}}{\Sigma_{\text{th}}} \right)^{-0.33}, & \Sigma_{\text{res}} < \Sigma_{\text{th}}, \\ \left(\frac{\Sigma_{\text{res}}}{\Sigma_{\text{th}}} \right)^{0.34}, & \Sigma_{\text{res}} > \Sigma_{\text{th}}, \end{cases} \quad (10)$$

with $\Sigma_{\text{th}} = 85 M_{\odot} \text{ pc}^{-2}$.

2.2. Nuclear star cluster collapse

A seed is formed at the center of the galaxy if the stellar mass of the NSC is larger than the critical mass of the NSC ($M_{\text{NSC}}^{\text{stellar}} > M_{\text{crit}}$). The critical mass is obtained under the condition that the collision time is equal to or shorter than the age of the system (t_H) and is given by (Vergara et al., 2023)

$$M_{\text{crit}}(r_{\text{NSC}}) = r_{\text{NSC}}^{\frac{7}{3}} \left(\frac{4\pi M_{\star}}{3\Sigma_0 t_H G^{\frac{1}{2}}} \right)^{\frac{2}{3}}, \quad (11)$$

where G is the gravitational constant, $\Sigma_0 = 16\sqrt{\pi} R_{\star}^2 (1 + \Theta)$, with $\Theta = 9.54((M_{\star} R_{\odot}) / (M_{\odot} R_{\star})) (100 \text{ km s}^{-1} / \sigma)^2$ the Safronov number (Binney & Tremaine, 2008), which depends on the velocity dispersion σ and M_{\star} and R_{\star} are the mass and the radius of a single sun-like star. The value of σ is obtained assuming a virialized system as

$$\sigma = \sqrt{\frac{GM_{\text{NSC}}^{\text{stellar}}(r_{\text{NSC}})}{r_{\text{NSC}}}}. \quad (12)$$

The age of the system (t_H) is assumed to be equal to the stellar mass-weighted age and is given by

$$t_H = \int_0^t (t - t') dt' \dot{M}_{\text{NSC}}^{\text{stellar}}(t') \int_0^t dt' \dot{M}_{\text{NSC}}^{\text{stellar}}(t'), \quad (13)$$

where $\dot{M}_{\text{NSC}}^{\text{stellar}}(t')$ is the star formation rate at time t' and t is the present time.

Furthermore, we introduce a free efficiency parameter ϵ_r and a threshold mass $M_{\text{threshold}}$. The ϵ_r parameter is introduced to rescale the radius used to compute the critical mass for the NSC. The mass threshold is required to avoid the formation of very low BH seeds. Specifically, the radius used to compute the critical mass is rescaled $r_{\text{NSC}} \rightarrow \epsilon_r r_{\text{NSC}}$, with $0 < \epsilon_r \leq 1$. This is motivated by observational and computational studies of young massive clusters with initial sizes less than

Table 1. Description of the parameters of the models run in GALACTICUS. The value of A_{res} is fixed in order not to exceed the maximum NSC mass observed.

Model	A_{res}	ϵ_r	ϵ_\bullet	$M_{\text{threshold}} [M_\odot]$
Model A	$1 \cdot 10^{-2}$	1.0	0.5	10^3
Model B	$1 \cdot 10^{-2}$	0.5	0.5	10^3
Model C	$1 \cdot 10^{-2}$	0.1	0.5	10^3

0.3 pc which can expand more than 10 times (Banerjee & Kroupa, 2017).

NSC forms a BH seed if $M_{\text{NSC}}^{\text{stellar}} > M_{\text{threshold}}$ and $M_{\text{NSC}}^{\text{stellar}} > M_{\text{crit}}$.

2.3. Simulations

We start from the best baryonic physics constrained model in GALACTICUS* and vary the relevant parameters for the evolution of the NSCs. The description of the parameters explored are available in Table 1. The mass for the threshold is set using the critical mass concept. This implicitly assumes that the stellar cluster is well-sampled and we assume here that it requires a minimum of at least around 1000 stars, changing this value indeed would extend the power-law to lower masses without affecting the high end very significantly.

The value of A_{res} is fixed in order to not exceed the maximum NSC mass observed at $z = 0$. The value is found to be $A_{\text{res}} \approx 1 \cdot 10^{-2}$ and is in agreement with the order of magnitude previously reported ($A_{\text{res}} \approx 10^{-2} - 10^{-3}$) by Antonini et al. (2015).

3. Results

We output galaxies with $M_{\text{NSC}}^{\text{stellar}} > 10^4 M_\odot$ at $z = 0$ in GALACTICUS as this is the lower NSC mass observed in Côté et al. (2006); Georgiev et al. (2016); Spengler et al. (2017) due to the resolution limit in observations. Furthermore, we classify the galaxies with bulge to total stellar mass ratio larger than 0.2 as early-type galaxies, and late-type otherwise (Graham & Worley, 2008).

The distribution of the effective radius is shown in Figure 1. We only show the results of Model A as Model B and C show the same distribution. We notice that the comparison between the observations of early- and late-type galaxies and models A, B, and C show that the most of the radii distribution is below 10 pc but it does not exclude the existence of NSCs with larger radii. However, our simulations underestimate the number of NSC with $r_{\text{eff,NSC}} < 5$ pc in early-type galaxies and overestimate the number of NSC in late-type galaxies.

In Figure 2 we show the stellar mass of the NSC as a function of the stellar mass of the host galaxy compared with the data from Spengler et al. (2017) (red dots) and Georgiev et al. (2016) (blue dots). The stellar mass of NSCs is slightly underestimated, this could be as result of the absence of another mechanism to form NSCs in the code.

*<https://github.com/galacticusorg/galacticus/wiki/Constraints:-Baryonic-Physics>

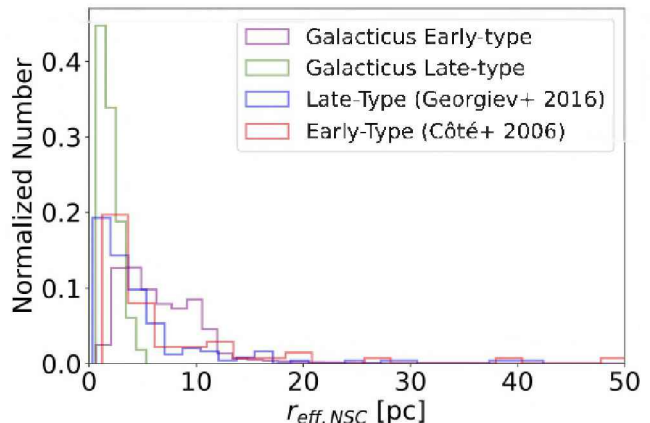


Fig. 1. Radii distribution of the observed NSCs compared with GALACTICUS. In both, the radii of most NSCs are below 10 pc. Data for early-type galaxies is taken from the ACSVCS survey Côté et al. (2006), and for late-type spiral galaxies from Georgiev et al. (2016). Adaptation from Neumayer et al. (2020).

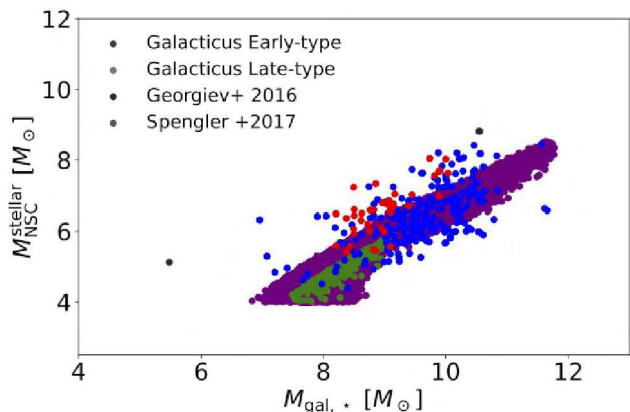


Fig. 2. Scaling relation between the stellar mass of the host galaxy and the stellar mass of the NSC. Purple dots represent the output of GALACTICUS at $z = 0$. Blue and red dots are observations from Georgiev et al. (2016) and Spengler et al. (2017), respectively.

In models A and B, there is no formation of BH seeds. However, Model C does form BH seeds with masses in the order of $10^3 M_\odot$ and $\sim 10^{5.5} M_\odot$ as shown in Figure 3. This suggests that the conditions to form a BH seed in this scenario are satisfied in initially more compact NSCs. The peak of the distribution is in BH seeds with masses $10^3 M_\odot$ and decreases as the BH mass increases.

4. Conclusions

The absence of another NSC formation scenario (e.g. globular cluster migration) could be the reason of the slightly underestimation of the stellar mass of NSCs predicted by GALACTICUS in Figure 2. This is expected according to the simulations of Antonini et al. (2015). The in situ star formation scenario contributes up to $\sim 80\%$ of the final stellar mass of the NSC in their simulations.

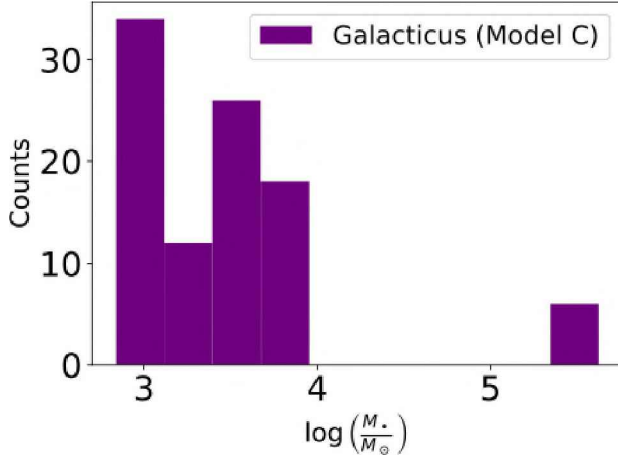


Fig. 3. Mass distribution of the black hole seeds formed in Model C. The mass range of formed seeds is from $10^3 M_\odot$ to $\sim 10^{5.5} M_\odot$. Models A and B do not form BH seeds as result of this mechanism.

Although our simulations recover a scaling relation between the stellar mass of the host galaxy and the stellar mass of the NSC, the inclusion of the globular cluster migration scenario (Antonini et al., 2015) could improve the agreement of our model with the observations.

From Figure 3, we conclude that the formation of BH seeds under this mechanism is possible if $\epsilon_r = 0.1$, suggesting that BH seeds are favored to form under this mechanism in initially more compact NSCs. This is consistent with studies of young massive clusters, which initially are more compact and increases their size due to external processes (Banerjee & Kroupa, 2017). In a future work we will explore if there is a critical limit for the value of ϵ_r where NSC could stop forming seeds as the clusters are more relaxed.

Acknowledgements: We gratefully acknowledge support by the ANID BASAL project FB210003, as well as via the Millenium Nucleus NCN19-058 (TITANs).

References

Antonini F., Barausse E., Silk J., 2015, *ApJ*, 812, 72

- Banerjee S., Kroupa P., 2017, *A&A*, 597, A28
 Benson A.J., 2012, *New Astronomy*, 17, 175
 Bentz M.C., Manne-Nicholas E., 2018, *ApJ*, 864, 146
 Binney J., Tremaine S., 2008, *Galactic Dynamics: Second Edition*, Princeton University Press
 Böker T., et al., 2002, *AJ*, 123, 1389
 Böker T., et al., 2004, *AJ*, 127, 105
 Côté P., et al., 2006, *ApJS*, 165, 57
 Durrell P.R., 1997, *AJ*, 113, 531
 Erwin P., Gadotti D.A., 2012, *Advances in Astronomy*, 2012, 946368
 Escala A., 2021, *ApJ*, 908, 57
 Ferrarese L., et al., 2006, *ApJL*, 644, L21
 Filippenko A.V., Ho L.C., 2003, *ApJL*, 588, L13
 Georgiev I.Y., et al., 2009, *MNRAS*, 396, 1075
 Georgiev I.Y., et al., 2016, *MNRAS*, 457, 2122
 Graham A.W., Worley C.C., 2008, *MNRAS*, 388, 1708
 Granato G.L., et al., 2004, *ApJ*, 600, 580
 Gültekin K., et al., 2009, *ApJ*, 695, 1577
 Haiman Z., Ciotti L., Ostriker J.P., 2004, *ApJ*, 606, 763
 Hoyer N., et al., 2021, *MNRAS*, 507, 3246
 Kormendy J., Ho L.C., 2013, *ARA&A*, 51, 511
 Krumholz M.R., 2012, *ApJ*, 759, 9
 Krumholz M.R., McKee C.F., Tumlinson J., 2009, *ApJ*, 699, 850
 Lapi A., et al., 2014, *ApJ*, 782, 69
 Natarajan P., Treister E., 2009, *MNRAS*, 393, 838
 Neumayer N., Seth A., Böker T., 2020, *A&A Rv*, 28, 4
 Neumayer N., Walcher C.J., 2012, *Advances in Astronomy*, 2012, 709038
 Neumayer N., et al., 2011, *MNRAS*, 413, 1875
 Nguyen D.D., et al., 2019, *ApJ*, 872, 104
 Pacucci F., Natarajan P., Ferrara A., 2017, *ApJL*, 835, L36
 Pechetti R., et al., 2020, *ApJ*, 900, 32
 Phillips A.C., et al., 1996, *AJ*, 111, 1566
 Reines A.E., Volonteri M., 2015, *ApJ*, 813, 82
 Rusli S.P., et al., 2013, *AJ*, 146, 45
 Sesana A., et al., 2014, *ApJ*, 794, 104
 Seth A., et al., 2008, *ApJ*, 678, 116
 Seth A.C., et al., 2010, *ApJ*, 714, 713
 Spengler C., et al., 2017, *ApJ*, 849, 55
 Vergara M.C., et al., 2023, *MNRAS*, 522, 4224
 Volonteri M., 2010, *A&A Rv*, 18, 279
 Wehner E.H., Harris W.E., 2006, *ApJL*, 644, L17